

its processing into other forms, including immobilized SEN-CA, etc. The synthesis protocol is versatile and can be employed for stabilizing other enzymes. This study illustrates the synthesis of SEN-CA by a simpler method and corroborates the findings of Kim and Grate<sup>5</sup> on armoured structures, with characteristics of enhanced stabilization of the enzymatic activity and reduced mass-transfer limitation relative to large-scale immobilization with the possibility of processability into additional forms, including hierarchical architectures. SEN-CA could be used to accelerate the hydration of CO<sub>2</sub> in biomimetic CO<sub>2</sub> sequestration in an aqueous solution. There is an improvement in the storage stability in the form of carbonation capacity of SEN-CA compared to free CA. It has been observed that SEN-CA retained 28% of its initial carbonation capacity up to 30 days.

1. Mirjafari, P., Asghari, K. and Mahinpey, N., Investigating the application of enzyme carbonic anhydrase for CO<sub>2</sub> sequestration purposes. *Ind. Eng. Chem. Res.*, 2007, **46**, 921–926.
2. Bond, G. M., Stringer, J., Brandvold, D. K., Simsek, F. A., Medina, M. G. and Egeland, G., Development of integrated system for biomimetic CO<sub>2</sub> sequestration using the enzyme carbonic anhydrase. *Energy Fuels*, 2001, **15**, 309–316.
3. Bhattacharya, S., Nayak, A., Schiavone, M. and Bhattacharya, S. K., Solubilization and concentration of carbon dioxide: novel spray reactors with immobilized carbonic anhydrase. *Biotechnol. Bioeng.*, 2004, **86**, 37–42.
4. Favre, N., Lorraine Christ, M. and Pierre, A. C., Biocatalytic capture of CO<sub>2</sub> with carbonic anhydrase and its transformation to solid carbonate. *J. Mol. Catal. B: Enzymatic*, 2009, **60**, 163–170.
5. Kim, J. and Grate, J. W., Single-enzyme nanoparticles armored by a nanometer-scale organic/inorganic network. *Nano Lett.*, 2003, **3**, 1219–1222.
6. Yan, M., Liu, Z., Lu, D. and Liu, Z., Fabrication of single carbonic anhydrase nanogel against denaturation and aggregation at high temperature. *Biomacromolecules*, 2007, **8**, 560–565.
7. Kim, J. *et al.*, Single enzyme nanoparticles in nanoporous silica: a hierarchical approach to enzyme stabilization and immobilization. *Enzyme Technol.*, 2006, **39**, 474–480.
8. Yadav, R., Labhsetwar, N., Kotwal, S. and Rayalu, S., Single enzyme nanoparticle for biomimetic CO<sub>2</sub> sequestration. *J. Nanopart. Res.*, 2010, DOI: 10.1007/s11051-010-0026-z.
9. Armstrong, J. M., Myers, D. V., Verpoorte, J. A. and Edsall, J. T., Purification and properties of human erythrocytes carbonic anhydrase. *J. Biol. Chem.*, 1966, **241**, 5137–5149.
10. Wilbur, K. M. and Anderson, N. G., Electrometric and colorimetric determination of carbonic anhydrase. *J. Biol. Chem.*, 1948, **176**, 147–154.
11. Yadav, R. *et al.*, Immobilized carbonic anhydrase for the biomimetic carbonation reaction. *Energy Fuels*, 2010, **24**, 6198–6207.
12. Ramanan, R., Kannan, K., Sivanesan, S. D., Mudliar, S., Kaur, S., Tripathi, A. K. and Chakrabarti, T., Bio-sequestration of carbon dioxide using carbonic anhydrase enzyme purified from *Citrobacter freundii*. *World J. Microbiol. Biotechnol.*, 2009, **25**, 981–987.
13. Mitra, M., Lato, S. M., Ynalvez, R. A., Xiao, Y. and Moroney, J. V., Identification of a new chloroplast carbonic anhydrase in *Chlamydomonas reinhardtii*. *Plant Physiol.*, 2004, **135**, 173–182.

**ACKNOWLEDGEMENTS.** We thank CSIR, New Delhi for funds under Supra Institutional Project [SIP-16 (4.2)], and also DBT [G-1-(1427)], New Delhi. We also thank Prof. Hata, Kyushu University, Japan for providing TEM image of SEN-CA.

Received 7 May 2010; revised accepted 18 November 2010

## Detection of potential site for future human habitability on the Moon using Chandrayaan-1 data

A. S. Arya\*, R. P. Rajasekhar,  
Guneshwar Thangjam, Ajai and  
A. S. Kiran Kumar

Space Applications Centre, Indian Space Research Organization,  
Ahmedabad 380 015, India

**Chandrayaan-1, the maiden Indian lunar spacecraft, carried 11 different scientific payloads on-board. The Terrain Mapping Camera (TMC) having 5 m spatial resolution and three-dimensional viewing capability had better sensor parameters than other similar cameras flown to the Moon before this mission. TMC captured the lunar surface features with unprecedented clarity. A buried, uncollapsed and near horizontal lava tube was detected in TMC stereo images of the Oceanus Procellarum area on the Moon. A Digital Elevation Model was generated to view the feature in three-dimensional perspective. A couple of rilles have been found to be connected sub-surficially by an undamaged lava tube, indicating that the roof of this section of the tube has remained intact since its formation. The lava tube has been analysed thoroughly in terms of morphometry, topography, surface composition and surface ages of the surrounding regions. Such a lava tube could be a potential site for future human habitability on the Moon for future human missions and scientific explorations, providing a safe environment from hazardous radiations, micro-meteoritic impacts, extreme temperatures and dust storms.**

**Keywords:** Human habitability, lava tube, Moon, rille.

CHANDRAYAAN-1, the maiden Indian planetary mission to the Moon, carried 11 different and complementary sensors on-board. One of the sensors was a panchromatic camera – the Terrain Mapping Camera (TMC). TMC image in the panchromatic spectral range of 0.5–0.75 μm with a stereo view in the fore, nadir and aft directions of the spacecraft movement and with a high spatial resolution of 5 m at an orbital height of 100 km (ref. 1), enable three-dimensional viewing of the lunar surface with crisp and clear surface features and morphology. The Digital Elevation Model (DEM) generated from the three look angles enables morphometric study of various lunar features, thus furnishing topographic relief and dimensions of various morphological entities. Identifying sites for permanent base stations for possible human settlements on the Moon is important for long-term perspective of lunar exploration. The absence of an atmosphere and intrinsic magnetic field make the lunar surface vulnerable

\*For correspondence. (e-mail: draryaas@gmail.com)

to impacts of meteorites or other bodies as well as energetic particles and radiations, making human settlement very difficult. Thus there is a need to identify locales, which have survived the onslaught of meteoritic impacts over ages and are also shielded from energetic particles, making them suitable for human settlement on the Moon. One such entity could be the volcanic tubes and rilles systems. A rille is a remnant of the volcanic tube, whose roof has capsized and a valley is created, and at places the roofs of such tubes do not collapse and remain intact, with a hollow interior in most cases.

Lava tubes are basically formed when an active low-viscosity lava flow develops a continuous and hard crust due to radiative cooling of its outermost part, which thickens and forms a solid roof above the still flowing lava stream beneath. At the end of the extrusion period, if the lava flow conditions were ideal in terms of viscosity, temperature, supply rate and velocity, an empty flow channel free from molten magma is left in the form of an approximately cylindrical shaped tunnel below the surface<sup>2,3</sup>. The suitability for a safe human base and habitability in a lava tube has been discussed earlier<sup>2-8</sup>. The basic idea for such a base and habitat is to provide safety from hazardous radiations, micro-meteoritic impacts, extreme temperatures and dust storms. An analysis of radiation safety issues on lunar lava tubes has been made by considering radiations from galactic cosmic rays (GCR) and solar particle events (SPE) interacting with the lunar surface, modelled as a regolith layer and rock<sup>2</sup>. In the simulation, the chemical composition has been chosen as typical of the lunar regions (Oceanus Procellarum) where the largest number of lava tube candidates are found and the results are as follows: (i) After 6 m depth, no effects of radiation due to or induced by GCRs are observable in the simulation; (ii) After less than 1 m, no effects of radiation due to or induced by SPE particles are observable; (iii) Natural or induced radioactivity does not play a significant role in the lava tube exposures; (iv) No significant differences in the results have been observed between the lunar night and the lunar day scenarios. Lava tubes provide a natural environmental control with a nearly constant temperature of  $-20^{\circ}\text{C}$ , unlike that of the lunar surface showing extreme variation, maximum of  $130^{\circ}\text{C}$  to a minimum of  $-180^{\circ}\text{C}$  in its diurnal cycle. Lava tubes offer a dust-free environment, which is also an essential condition. In addition, adapting lava tubes for human use requires minimal construction, effectively and economically. Another idea proposed is that the sheltered environment and consistently cold temperatures in the lava tubes may serve as a trap for water ice and other volatiles<sup>9</sup>. Regarding roof thickness and safety, one view is that in order to confine one atmosphere of internal pressure, static roof thickness must be at least 16 m (ref. 10). Lava tubes will be important to scientists and planetary exploration architects for a number of reasons, and the effort required to discover and characterize them

offers the opportunity for synergy and the multi-purposing of tools, manpower and mission planning, discussing in detail various aspects<sup>5</sup>: (i) To the geologist, discovering and gaining entry to a section of the uncollapsed lava tube would permit direct examination of pristine bedrock, and potentially, materials brought up from depths that are inaccessible from the surface. This could show, in context, undisturbed native mineral composition as it flowed up from the lunar interior. It would be isolated from solar wind deposition and gardening, transported ejecta, asteroidal and cometary deposition, and mixing with shock-modified materials. (ii) Lava tubes are also useful in understanding the history of volcanism as well as the thermal history of a planet or Moon. (iii) The same bedrock would also be an ideal location to conduct seismic investigations. Thus lava tubes are not only a safe natural cavity, but also a readymade structure for a lunar base, being a habitat. Regarding the present lava tube under study, geographically it is located in the Oceanus Procellarum, equatorial region of nearside. Oceanus Procellarum is also an interesting and important mare region having complex volcanic constructs like Marius Hills Complex, Aristarchus Plateau, etc. and correspondingly distinct thermal history with various ranges of basaltic samples, including Procellarum KREEP basalts, and different lunar morphological features like rilles, domes, cones, scarps, ridges, ray craters, and Reiner Gamma formation. Thus it is important to study in detail the pros and cons of the suggested lava tube.

Lava tubes are also found on the Earth's surface. Field observations<sup>4</sup> of several volcanic terrains on Earth, especially in the Hawaii islands, indicate that the majority of lava tubes remain partially void, that is, less than 30% of the tubes have been (partially) filled by later flows. Less than 1% of the lava tubes observed in the field are completely filled by later flows (e.g. Makapu'u Tube, Oahu, Hawaii). Of the several hundred lava tubes known to exist on and around Kilauea, more than 90% are open or void and less than 30% of the tubes have been filled in by later flows. In tubes that have been partially filled, the lava toes extend inward from the tube walls. Other evidence, derived from the study of lunar volcanic features, suggests that not all lunar tubes are plugged with concealed lava and that void lava tubes exist on the Moon, and many basaltic lava flows and channels exist on the lunar surface<sup>11-15</sup>. These may include the discontinuous series of rilles aligned along their strike. There could be lava caves between the rilles, which may be hollow.

In the present study, one such tube has been identified in the Oceanus Procellarum, to north of Rima Galilaei above the lunar equator using Chandrayaan-1 images. The location of the study area on the nearside of the Moon is shown as a rectangular box (red) on the panchromatic image (Figure 1) taken by India's Cartosat-2A satellite. Major mare basins and prominent craters are also shown in this image. TMC multi-look capability has been used

to derive DEM of the study area and subsequently to generate orthoimage from satellite stereo images using photogrammetric technique<sup>16</sup>, which is free from all geometric distortions including relief displacement.

The rille and the adjoining areas have been systematically studied for morphometry and its dimensions using TMC-DEM, and for surface compositional variations using Hyper Spectral Imager (HySI). For this study, both orthoimage and DEM (orbit-798) acquired on 13 January 2009, at an orbital height of 100 km were used. Topographic profiles, both across and along the lava tube were studied.

TMC orthoimage of the area surrounding the rille is shown in Figure 2a. A three-dimensional perspective view of the smaller region around the rille is prepared by superimposing DEM over the orthoimage (Figure 2b). This gives a fairly good idea about the elevation/depth variations in and around the rilles. It clearly shows the two wedge-shaped rilles and the uncollapsed area between them. The areas considered for age determination both above and below the rille are outlined as red boxes I and II respectively (Figure 2a). The width of the image shown in Figure 2a and b is 20 and 6.6 km respectively. The main rille appears like a cobra-hood and runs for about 3.9 km in the NE-SW direction. There is another small rille, about 1.9 km SW of the existing rille, which appears to be an extension of this tube, whereas the

intermittent stretch between the two rilles seems to be a near-flat roof of an underground lava tube which did not collapse. TMC stereo data have been analysed to find the length, depth and slope using cross-sectional profiles along and across this rille to establish continuity between the main rille and the shorter rille. The values of the contours are taken from a relative DEM generated with reference to a lunar radius of 1737.2 km. It is observed that the altitudinal drop between the two rilles, along the common strike, is about 85 m (–1317 to –1230 m). This suggests that the smaller rille is lower than the main rille, thus suggesting a continuity of the main rille in the SW direction. The length of the smaller rille is about 1.9 km and topography along this section varies from approximately –1300 to –1350 m. It is to be noted that the altitudinal drop along the rille, is not the actual depth of the rille, since it presumably contains the collapsed roof of the rille, well.

A colour-coded contour map around the lava tube/rille has been generated using TMC-DEM (Figure 3). This map shows relative elevations indicating variations of –1120 to –1360 m in the study area. The overall topography shows a decreasing slope from ESE to WNW of about 150 m (–1150 to –1300 m depth). This rules out any possibility of lava flow from the western side filling the portion between the two rilles after their emplacement. Thus, the remaining portion between the two rilles is the uncollapsed roof of the same lava tube rather than post-rille lava filling. This lava tube, in all probability, as in the case of lava tubes on Earth, is a strong candidate which conceals a hollow cave.

Orthoimage and DEM have been used to compute the dimensions of the above tube/rilles. Total length of the entire rille, including the intermittent uncollapsed lava tube, along its central portion, is approximately 7.36 km and altitude varies from –1358 to –1200 m from NE to SW. A topographic profile along this entire rille/uncollapsed tube was also analysed in detail. The diameter of the assumed cylindrical tube as computed from DEM is 120 m. The approximate surface area of the entire rille is computed to be about 2.77 km<sup>2</sup> and volume is 0.08 km<sup>3</sup>. The length of the uncollapsed portion is found to be 1.72 km; the approximate surface area and the volume are computed to be 0.65 km<sup>2</sup> and 0.02 km<sup>3</sup> respectively. The portion above this uncollapsed tube, exposed on the lunar surface (red box, in Figure 3) is approximately 360 m wide and 1.7 km long. Surface topography along the uncollapsed portion varies from –1317 to –1230 m in relative height.

The roof thickness of the uncollapsed portion of the lava tube is estimated using the empirical relation of crater geometry<sup>2</sup>

$$t = d \times 0.25 \times 2,$$

where  $t$  is the estimated thickness of the tube segment,  $d$  the maximum crater diameter superposed on the tube

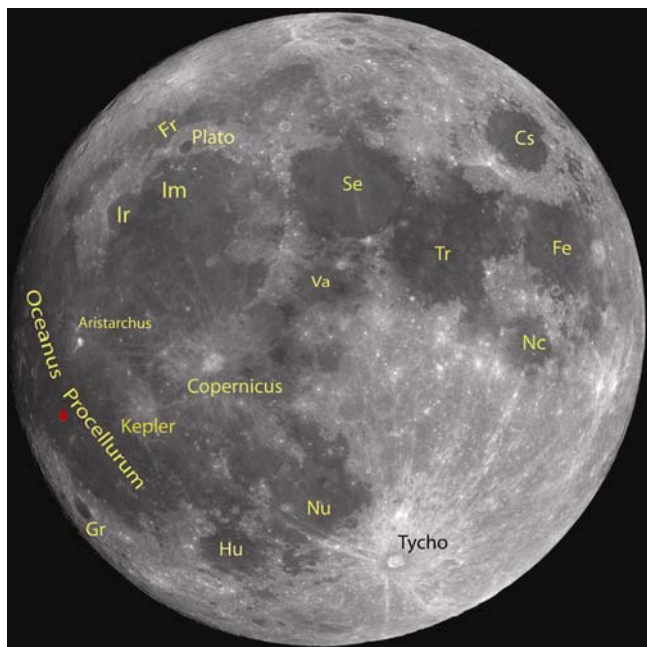


**Figure 1.** Cartosat-2A satellite panchromatic image of nearside of the Moon showing the location of the study area as a rectangular box (red) in Oceanus Procellarum on the western nearside. Also shown are the major mare basins (Fr, Mare Frigoris; Im, Mare Imbrium; Ir, Sinus Iridum (a lunar bay); Hu, Mare Humorum; Nu, Mare Nubium; Nc, Mare Nectaris; Fe, Mare Fecunditatis; Cs, Mare Crisium; Se, Mare Serenitatis; Va, Mare Vaporum; Tr, Mare Tranquillitatis and Gr, Grimaldi basin) and the prominent craters (Plato, Aristarchus, Copernicus, Kepler, Tycho).

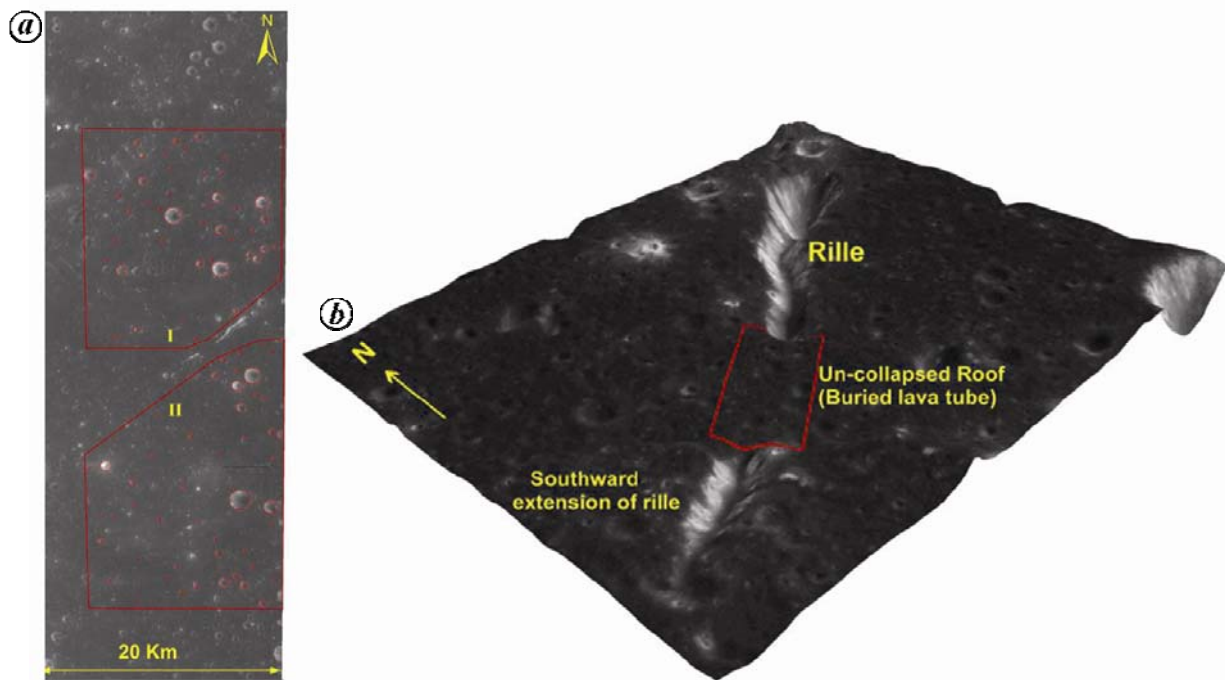


**Figure 2.** *a*, Segment of orthoimage, Terrain Mapping Camera orbit-798 showing the lunar lava tube, the red boxes I and II being the areas considered for age determination. *b*, Detailed three-dimensional perspective view (vertical exaggeration factor of 1.5) of the rille showing uncollapsed portion (red box).

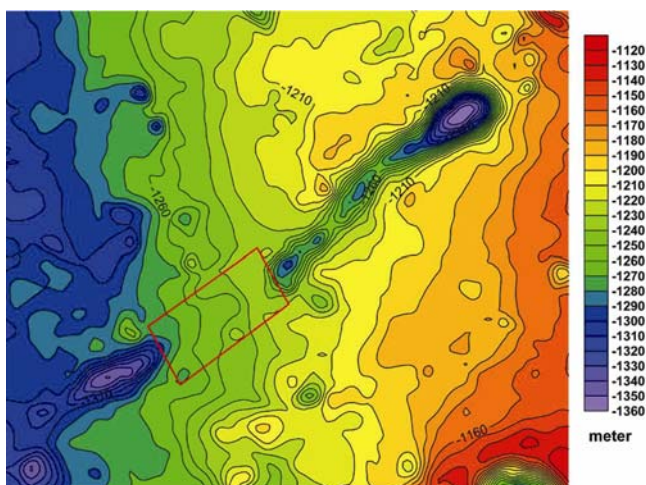


**Figure 3.** Colour-coded contour map of the study area showing the rille and uncollapsed portion of the lava tube (red colour box).

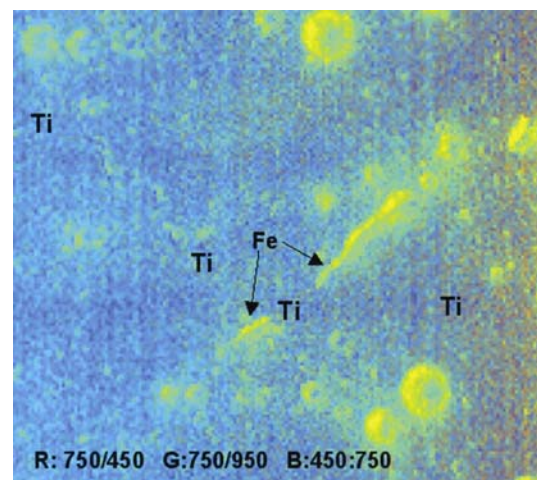


**Figure 4.** HySI image (FCC) of selected ratio bands showing the surface composition.

segment. Thus the maximum depth is approximately one-quarter the crater diameter ( $0.25 \times d$ ), and the roof thickness is at least twice the depth.

Again, the ratio of roof thickness ( $T_r$ ) of terrestrial lava tubes relative to typical dimensions of tube cross-section ( $T_c$ ) ranges from 0.25 to 0.125, and this estimate is in agreement with the lunar lava tubes<sup>4,11</sup>.

Here, the maximum crater diameter on the uncollapsed portion of the lava tube is 140 m. The roof thickness estimated is 70 m (ref. 2). The cross-section of the uncol-

lapsed portion of the lava tube is approximately 360 m, in which the roof thickness is in the range 45–90 m (refs 4, 11). The roof thickness derived using previous relation is in good agreement with this range and other similar studies<sup>2,4,7,11</sup>.

Surface compositional study has also been carried out using HySI data. HySI is a multi-spectral resolution camera and has 64 contiguous bands in the spectral range 0.4–0.95  $\mu\text{m}$ . The data available are 80 m spatial sampled with 20 km swath coverage from 100 km altitude<sup>17</sup>.

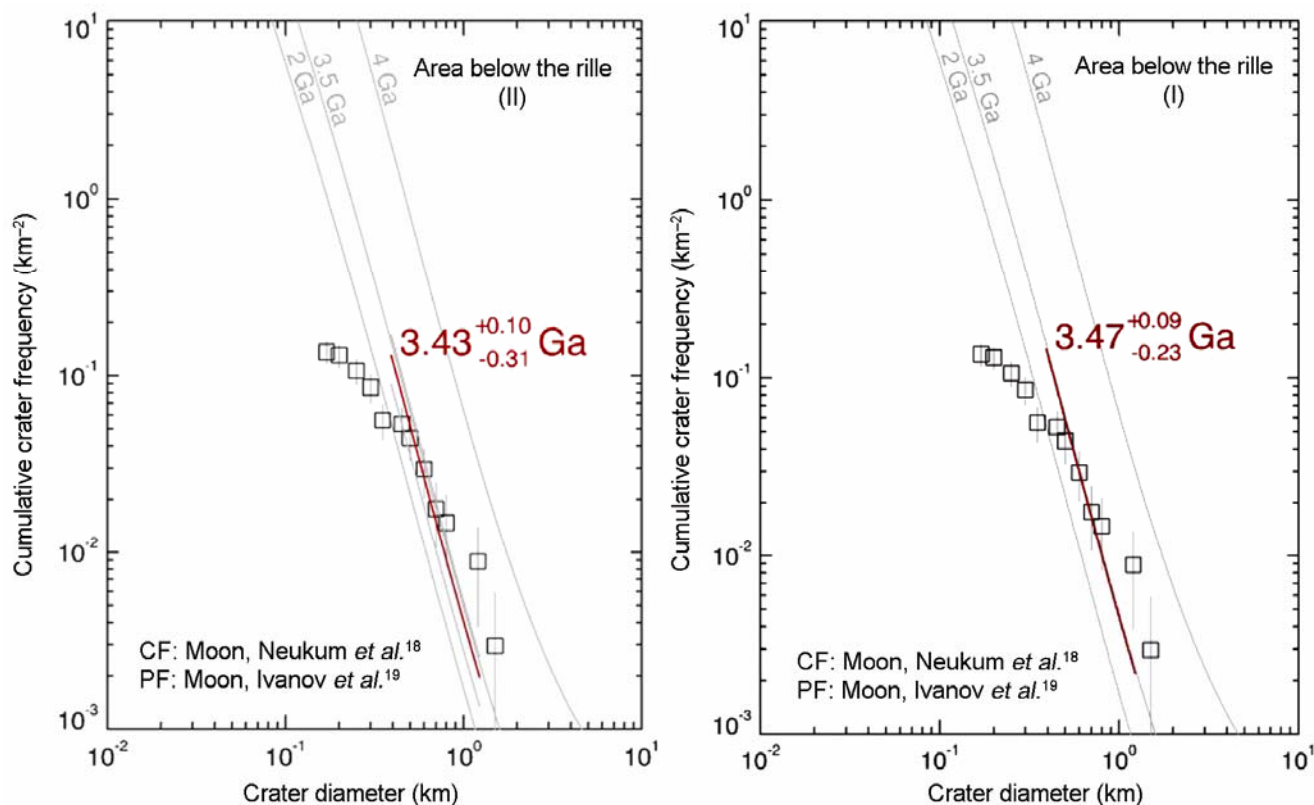


**Figure 5.** Cumulative crater size frequency plot for the selected areas shown in Figure 2a corresponding to areas I and II, above and below the rille respectively. PF, Production function; CF, Chronology function.

Spectral reflectance measurements of the lunar surface are sensitive to the mineralogy, mineral chemistry and physical state of the regolith, including the important optical effects of space weathering.

In the present study, three HySI bands, viz. 450, 750 and 950 nm have been used for generation of ratio images. Ratio of 450–750 nm is sensitive for mapping titanium. Similarly, ratio of 750–950 nm has been used for iron mapping and ratio of 750–450 nm basically shows the presence of plagioclase feldspar and or ejecta material. Ratio FCC of the lunar surface has been generated using the following band combinations

R: 750/450; G: 750/950; B: 450/750.

Therefore, in the ratio FCC, iron rich surfaces appear green to yellow, titanium-rich surfaces appear blue and ejecta deposits appear red/orange.

Surface mineral composition map of the study area is shown in Figure 4. The dominance of basalts, i.e. titanium and iron outside and inside the rilles respectively can be observed. This clearly shows the compositional homogeneity between the uncollapsed part of the rille system and the surrounding area. It further indicates that the portion between the above-mentioned two rilles is the uncollapsed roof of the underlying lava tube and thus the

possibility of the secondary lava flow filling the portion between the two rilles is ruled out.

In order to further rule out the above in terms of the surface ages of south and north of this rille/lava tube, the ages of these surface units were computed using crater-counting technique. The method of determining absolute ages for cratered planetary surface units has been discussed earlier<sup>18–21</sup>. This method is based on the fact that the flux and size of impact craters are a function of time. These methods have been validated using the age of samples returned from the Moon<sup>20,21</sup>. The concept is to fit the observed crater size–frequency distribution (SFD) of a given surface unit to a known crater production function (PF), and to use the crater frequency for certain crater sizes together with a calibrating chronology function to obtain an absolute age. PF describes how many craters of a given size are formed in relation to the number of any other size. It is determined by considering the crater SFDs of homogeneous surface units of the Moon or Mars. Since the oldest units are best characterized in age by the larger range of crater sizes and younger units by lesser craters, to construct PF for the entire observable diameter range, it is necessary to use a piecewise normalization procedure. Here, the crater diameters were measured as precisely as possible from the orthoimage of the TMC data within homogeneous geological units. Measured

crater diameters were plotted onto crater SFD curve using 'craterstat' IDL subroutine, which contains coefficients for Moon chronology and production functions<sup>18-21</sup>. Fitting the observed points with lunar production curve, as small segments, yielded the age of the lunar surface under study (Figure 5).

From the above method, the age of the northern (I) and southern parts (II) of the rille has been found to be 3.47 and 3.43 Ga respectively, which is nearly the same, given the margin of error as shown in Figure 5. This clearly rules out the possibility of differential emplacement of the mare basalts in the two distinct parts of the study area.

Chandrayaan-1 TMC and HySI data have been useful to detect and analyse lunar lava tubes/uncollapsed rilles in terms of morphology, morphometry, chronology and surface composition. For one particular system, the data were useful in systematically ruling out any possibility of secondary lava plugging the portion between the main rille and its southern extension. This underground lava tube is the uncollapsed portion between the two rilles and is suitable for future human habitat as it provides shelter from the impacting bodies, protects from direct exposure to extreme temperature conditions, dust storms, energetic particles and radiations of solar and galactic origin and also surface radioactivity. High-resolution TMC data and HySI data can be further used to study more such structures on the lunar surface.

11. Oberbeck, V. R., Quaide, W. L. and Greeley, R., On the origin of lunar sinuous rilles. *Mod. Geol.*, 1969, **1**, 75–80.
12. Cruikshank, D. P. and Wood, C. A., Lunar rilles and Hawaiian volcanic features: possible analogues. *Moon*, 1972, **3**, 412–447.
13. Masursky, H., Colton, G. W. and El-Baz, F., Apollo over the Moon: a view from orbit. NASA SP-362, 1978, p. 255.
14. Schaber, G. G., Boyce, J. M. and Moore, H. J., The scarcity of mappable flow lobes on the lunar maria: unique morphology of the Imbrium flows. Proc. Lunar Sci. Conf. 7th, 1976, pp. 2783–2800.
15. Greeley, R. and King, J. S., Volcanism of the Eastern Snake River Plain, Idaho: A Comparative Planetary Geology Guidebook. NASA CR-154621, 1977, p. 308.
16. Srivastava, P. K., Gopala Krishna, B. and Amitabh, Exploring the Moon in three dimension. *Coordinates*, 2009, **V(4)**, 6–10.
17. Chauhan, P. and Bhattacharya, S., Remote sensing of lunar surface composition using Chandrayaan-1 HySI data. In Geomatics, Pre-Conference Tutorial on 'Planetary Geomatics', Ahmedabad, 2–3 February 2010.
18. Neukum, G., Ivanov, B. A. and Hartmann, W. K., Cratering records in the inner solar system in relation to the lunar reference system. *Space Sci. Rev.*, 2001, **96(1/4)**, 55–86.
19. Ivanov, B. A., Mars/Moon cratering rate ratio estimates. *Space Sci. Rev.*, 2001, **96(1/4)**, 87–104.
20. Michael, G. G. and Neukum, G., Planetary surface dating from crater size–frequency distribution measurements: partial resurfacing events and statistical age uncertainty. *Earth Planet. Sci. Lett.*, 2010, **294**, 223–229.
21. Hiesinger, H., Jaumann, R., Neukum, G. and Head, J. W., Ages of mare basalts on the lunar nearside. *J. Geophys. Res.*, 2000, **105**, 29239–29275.

1. Kiran Kumar, A. S. *et al.*, Terrain mapping camera: a stereoscopic high-resolution instrument on Chandrayaan-1. *Curr. Sci.*, 2009, **96**, 492–496.
2. Hörz, F., Lava tubes: potential shelters for habitats. In *Lunar Bases and Space Activities of the 21st Century* (ed. Mendell, W. W.), Lunar and Planetary Institute, Houston, 1985, pp. 405–412.
3. Angelis, G. D., Wilson, J. W., Cloudsley, M. S., Nealy, J. E., Humes, D. H. and Clem, J. M., Lunar lava tube radiation safety analysis. *J. Radiat. Res. Suppl.*, 2002, **43**, S41–S45.
4. Coombs, C. R., Hawke, B. R. and Wilson, L., Kauhako crater and channel, Kalaupapa, Molokai: a terrestrial analog to Lunar Sinuous rilles. In Proceedings 20th Lunar Planet Science Conference, 1989, pp. 195–206.
5. Andrew, W. D. *et al.*, Lunar and Martian lava tube exploration as part of an overall scientific survey. Annual Meeting of LEAG, No. 2065, 2009.
6. Mardon, A. A., Lunar lava tubes and artificial tunnels: habitations for the near term future. *LPS*, 1997, **XXVIII**, 1023.
7. Bennett, S. A. and Carpenter, P., Lava tubes in the Alba Patera region of Mars: future human habitats and incubators of life? *Geol. Soc. Am. Abstr. Progr.*, 2009, **41(4)**, 51.
8. Clifford, S., Lava tubes and their potential as base sites for human exploration of Mars, 1997; <http://www.argoverse.com/LAVATUBE.html>
9. Billings, T. L., Radar remote sensing of lunar lava tubes from Earth. *J. Br. Interplanet. Soc.*, 1991, **44**, 255–256.
10. Kuck, D. L., Finding and utilizing lunar lava tubes. In Arizona University, Resources of Near-Earth Space: Abstracts (SEE N91-26019 17-91), SAO/NASA ADS Astronomy Abstract Service, 1991, p. 18.

**ACKNOWLEDGEMENTS.** We thank Dr R. R. Navalgund, Director, Space Applications Centre, Ahmedabad for his interest and guidance and Prof. J. N. Goswami, Director, Physical Research Laboratory, Ahmedabad; Dr P. K. Srivastava, DD-SIPA; Dr P. K. Pal, GD-AOSG; D. R. M. Samudraiah, DD-SEDA and Dr J. S. Parihar, DD-EPISA for useful comments and discussions. A.S.A. thanks Dr Carle Pieters, Brown University, USA for valuable suggestions during the early stages of this study. We also thank SPDCG/SIPA for providing TMC images and DEM; Greg Michael, Freie Universitat, Berlin, for help in applying the crater counting methodology, and the two anonymous reviewers for their constructive remarks that helped improve the manuscript.

Received 9 August 2010; revised accepted 2 December 2010